RSC Advances

ROYAL SOCIETY OF CHEMISTRY

www.rsc.org/advances

Self-assembled multimicellar vesicles via complexation of a rigid conjugated polymer with an amphiphilic block copolymer

Anbazhagan Palanisamy and Qipeng Guo*

Polymers Research Group, Institute for Frontier Materials, Deakin University, Locked Bag 2000, Geelong, Victoria 3220, Australia.

We report here a facile method for fabrication of multimicellar vesicles from self-assembled complexes of a flexible coil-like block copolymer and a rigid rod conjugated homopolymer.

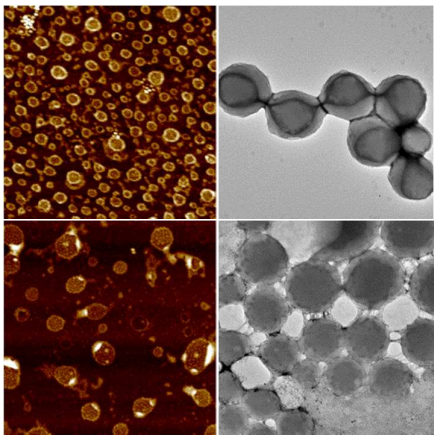

Journal Name

RSCPublishing

ARTICLE

Self-assembled multimicellar vesicles via complexation of a rigid conjugated polymer with amphiphilic block copolymer

Cite this: DOI: 10.1039/xoxxoooooox

Received ooth January 2012,
Accepted ooth January 2012

DOI: 10.1039/xoxxoooooox

www.rsc.org/

Anbazhagan Palanisamy and Qipeng Guo*

A viable method of encapsulating block copolymer micelles inside vesicles using a conjugated polymer is reported in this study. Self-assembly and complexation between a amphiphilic block copolymer poly(methyl methacrylate)-*b*-poly(acrylic acid) (PMMA-*b*-PAA) and a rod-like conjugated polymer polyaniline (PANI) in aqueous solution were studied using transmission electron microscopy, atomic force microscopy and dynamic light scattering. The complexation and morphology transformation were driven by electrostatic interaction between PANI and PAA block of the block copolymer. Addition of PANI to PMMA-*b*-PAA induced the morphology transformation from micelles to irregular vesicles through vesicles, thick-walled vesicles (TWVs) and multimicellar vesicles (MMVs). Among observed morphologies, MMVs were observed for the first time. Morphology transformation was studied as a function of aniline/acrylic acid molar ratios ([ANI]/[AA]). Micelles were observed for pure block copolymer, while vesicles and TWVs were observed at [ANI]/[AA] = 0.1, 0.3 respectively. MMVs were observed at [ANI]/[AA] = 0.5 and irregular vesicles observed for molar ratios at 0.7 and above. Clearly, a conjugated polymer like polyaniline can induce the morphology transformation even at its lower concentrations and produce complex morphologies.

Introduction

Amphiphilic block copolymers self-assemble into a variety of morphologies in aqueous media or mixed organic solvents depending on their composition and architecture.[1] Potential applications of these self-assembled systems in various fields, such as cosmetics, biomedicine, chemical process, catalysis, agro-chemicals[2-5] demands morphology control, as their bulk physical properties depend on molecular assemblies. Advanced polymerization techniques such as anionic or living radical polymerization were used to synthesize block copolymers of complex molecular architectures to tune their self-assembly.[6] For instance, Eri Yoshida have studied polymerization-induced self-assembly of an amphiphilic random block copolymer (poly(methyl methacrylate)-*b*-poly(methyl methacrylate-random-methacrylic acid)) in aqueous methanol solution.[7, 8] Various morphologies including giant vesicles were observed upon changing the hydrophobic-hydrophilic ratio,[9] and detailed mechanism of morphology transformation were also reported.[10] In parallel to these synthetic methods, morphology control has also been achieved through polymer complexation via non-covalent interactions,[11] varying solution conditions,[12] and adding ions[13]. Through judicious selection of polymer components, non-covalent interactions such as hydrogen bonding,[14] metal coordination[15] can be utilized to produce polymer complexes leading to various morphologies and bypass the need to synthesize a specific block copolymer each time.

Inspired from biological macromolecular assemblies, hydrogen bonding[16-18] in combination with ionic interaction, Van der Waals interaction and hydrophobic interaction were explored for polymer complexation studies. For flexible coil-like copolymer/homopolymer, copolymer/copolymer complexes, a sophisticated control over the morphology have been demonstrated both in bulk[5, 16] and in solution.[19] However, the complexation and self-assembly behaviour of flexible copolymers with rod-like homopolymers need to be explored. Unlike traditional coil type polymers, rod-like polymers aggregate into liquid-crystalline domains and produce distinctly different morphologies.[20] Most of the natural or synthetic materials such as helical proteins, polysaccharides, microtubules, polyamides, polyisocyanates, etc. adopt self-assembled rigid chain conformations to be a functional structure.[21] Incorporation of these rigid polymers into flexible block copolymer through complexation may exhibit rich self-assembly behaviour.

Conducting polymers are blended with flexible polyelectrolytes to overcome their inherent disadvantages such as rigidity and solubility.[22] Heteroatomic conducting polymers such as polypyrrole (PPY), polyaniline (PANI), poly (3, 4-

ethylenedioxythiophene) (PEDOT) etc. can form interpolyelectrolyte complexes (IPECs) with homopolymers or block copolymers in solution.[23] These blending components carry oppositely charged sequences that interact via electrostatic interaction to form IPECs. PANI/polyelectrolyte complexes have been extensively studied due to their ease of synthesis, facile redox and pH switching behaviour, high environmental stability and potential applications. Semi oxidized PANI emeraldine base (PANI-EB) was the most useful and soluble form of polyaniline studied for complexation with polyacid. Rubner and co-workers prepared electrically conductive multi-layered thin films by exploiting the electrostatic interaction between PANI-EB and polyelectrolytes.[24] Tripathy and co-workers reported helical conformation of PANI in presence of DNA as polyelectrolyte template to form an intermolecular complex. The unique DNA/PANI complex has been used to reversibly control the conformation of DNA double helix.[25] Amphiphilic block copolymers containing an anionic polyelectrolyte block and a neutral hydrophobic block has been used as micellar templates for preparing conducting polymer nanoparticles in an aqueous medium or in mixed solvents. Morphology of these nanoparticles was dictated via block copolymer micelles as templates.[22]

More complex and fascinating nanostructures have been prepared in dilute solution using conducting polymer as one of the self-assembling components. Mathieu and co-workers identified self-assembled chiral supramolecular structures via electrostatic binding of DNA and conjugated polymer.[26] Solution self-assembly of rod-coil block copolymers yielded helical superstructures[27], spherical, rod-like[28] and fibre-like micelles.[29] Formation of liquid-crystalline domains in conjugated polymers due to π-π stacking interaction provides unique self-assembly behaviour. For instance, spherical micelles and thin-layered vesicular aggregates were observed in an oligoaniline containing triblock copolymer.[30] Typically, studies involving PANI/block copolymer complexes addressed PANI solubility, conductivity and processability issues in solid state.[31, 32] Up to now, the self-assembly and morphology of PANI/block copolymer complexes in a selective solvent still remain unexplored.

Herein we report the aggregate morphologies of IPECs formed between block copolymer poly(methyl methacrylate)-*block*-poly(acrylic acid) (PMMA-*b*-PAA) and homopolymer polyaniline (PANI) in an aqueous milieu. The block copolymer can readily self-assemble into nanostructures in aqueous solution owing to hydrophobicity of PMMA block and hydrophilicity of PAA block. Electrostatic interaction between PANI and PAA block was accounted for morphology change in self-assembled aggregates at various [ANI]/[AA] molar ratios. A similar work has been reported by Dmitry et al. on formation of water-soluble micellar IPECs from flexible amphiphilic block copolymer/homopolymer mixture.[33] However, we have used a rigid-rod conjugated homopolymer to form IPECs with a flexible block copolymer, and in addition, morphology evolution have been systematically investigated at various compositions and studied using transmission electron microscopy (TEM), atomic force microscopy (AFM), dynamic light scattering (DLS), Fourier transform infrared spectroscopy (FTIR) and UV-visible spectroscopic techniques. Spherical micelles, vesicles, thick-walled vesicles (TWVs), multimicellar vesicles (MMVs) and irregular vesicles were observed at different compositions. A simple and viable method of preparing compartmentalized vesicles using conjugated polymer is introduced in this study. Compartmental vesicles and micelles have gained attention in recent years due its potential applications in various areas.[34]

Experimental section

Materials

Polyaniline emeraldine base (PANI-EB) and polyacrylic acid (PAA) were purchased with an average molecular weight Mw of 5000 and 10000 from Aldrich Chemical Co., Inc. respectively. The block copolymer PMMA-*b*-PAA with Mn (PMMA) = 41000, Mn (PAA) = 10000 and Mw/Mn = 1.20 was purchased from Polymer Source, Inc. All the polymers were used as received. Reagents were of analytical grade and used without further purification.

Transmission Electron Microscopy (TEM)

TEM experiments were performed on a JEOL JEM-2100 transmission electron microscope operating at an acceleration voltage of 100 KV. Aqueous solution of complex aggregates was deposited onto a carbon coated copper EM grid, after one minute, excess solution was removed using a piece of filter paper. Then, copper grids were dried at room temperature and negative staining performed using a 1% (w/v) aqueous uranyl acetate solution. The samples containing PANI were vapour stained using osmium tetroxide (OsO4) in addition to uranyl acetate staining.

Atomic Force Microscopy (AFM)

The AFM measurements of complex aggregates were performed on a Bruker Multimode™ 8 SPM instrument. Thin film of samples was prepared by casting aqueous solution of complexes on a silicon substrate using a spin coater at 3000 rpm followed by drying at room temperature. The sample surface was probed using a silicon cantilever (spring constant of 42 N/m) in tapping mode at room temperature. The height images were recorded and analyzed using NanoScope Analysis software.

Dynamic Light Scattering (DLS)

The hydrodynamic diameter of IPECs was measured on a Malvern Zetasizer Nano ZS spectrometer equipped with 633 nm He-Ne laser. The measurements were performed at 25 °C with a detection angle of 173°. The scattering intensity autocorrelation functions from the digital correlator were analyzed using Cumulant method to derive size and size distribution of complex aggregates.

Fourier Transform Infrared (FTIR) Spectroscopy

The FTIR spectra of the samples were recorded using a Bruker Vertex-70 FTIR spectrometer. The samples were dried in

vacuum for 48 hours, grounded with KBr and prepared into disks. The FTIR measurements were performed in a moisture free condition by the average of 32 scans in the standard wavenumber range 600-4000 cm^{-1} at a resolution of 4 cm^{-1}.

UV-visible spectroscopy

The UV-visible spectra were recorded using a Varian Cary UV-visible spectrophotometer in the wavelength range of 300-800 nm. The aqueous solutions of polymer complexes were used to record the absorption spectra.

Results and discussion

Interpolyelectrolyte complexes

Block polyelectrolytes with charged hydrophilic block and neutral hydrophobic block can self-assemble into various core-shell-corona structures in an aqueous milieu. Adding an oppositely charged homopolymer to a block polyelectrolyte can form self-assembled water soluble complex species. The insoluble neutral block forms core, while the IPEC forms the shell. The whole structure is solubilized in water by the shell forming polyelectrolyte block that does not involve in complexation. Since IPECs are formed via electrostatic interaction between oppositely charged species, these aggregates are sensitive for pH, temperature, solvent composition and ionic strength of the medium.[35]

In this study, both the block copolymer PMMA-*b*-PAA and homopolymer PANI were dissolved separately in a common solvent tetrahydrofuran (THF) to obtain 0.5% (w/v) and 0.1% (w/v) polymer solutions respectively. PANI solution was sonicated for one-hour post stirring to aid complete dissolution. Polymer solutions were filtered using 0.45 μm nylon filters to remove any residues if present. Then PANI-THF solution was added drop wise into PMMA-*b*-PAA solution at predetermined compositions to prepare IPECs. The compositions were expressed as molar ratio of polyaniline concentrations to the concentration of poly(acrylic acid) ([ANI]/[AA]) ranging from 0.1 to 0.7 and the corresponding weight ratios ranging from 0.02 to 0.16. Then deionized water was added drop wise up to 29 wt % into these complexes under stirring condition to induce aggregation. After 12 hours of continuous stirring, water addition continued till 50 wt %, and complexes were quenched by adding excess water (70 wt %). Finally, the complex aggregates were dialyzed against deionized water for 72 hours to remove the common solvent THF. As prepared IPECs were used for further experiments.

The PMMA-*b*-PAA/PANI compositions used in this study were chosen based on the solubility of PAA/PANI homopolymer complexes in water. To estimate the solubility, PAA homopolymer of similar molecular weight to that of the PAA block of PMMA-*b*-PAA and PANI were dissolved in THF individually. Mixtures of various molar ratios of aniline to acrylic acid ranging from 0.1 to 2 were prepared and transferred into water via dialysis. The PANI/PAA complexes with [ANI]/[AA] compositions less than 0.8 were stable, while macroscopic aggregation was observed for compositions greater than 0.8. Macroscopic aggregation was visually confirmed and also using DLS method, which implies, the complexes are stabilized at lower PANI concentrations by the fraction free PAA chains dissolved in water. At higher PANI concentrations, the PAA chains may be collapsed to form macroscopic precipitates due to limited solubility in water. Hence, [ANI]/[AA] compositions less than 0.8 were used to study the self-assembly behaviour of PMMA-*b*-PAA/PANI complexes.

Here, the homopolymer PANI acquires a positive charge due to protonation in acidic medium and forms complex with PAA block of the block copolymer (Figure 1). Meanwhile, PAA is a weak acid with a lower degree of ionization, and its dissociation is further limited in low dielectric solvent such as THF[36]. Addition of PANI to this block copolymer/THF solution may not induce effective complexation. Thus, addition of water to this block copolymer/PANI mixture plays two important roles: a) acts as a poor solvent for PMMA and trigger aggregation, b) induce complexation via ionizing PAA thereby protonating PANI.

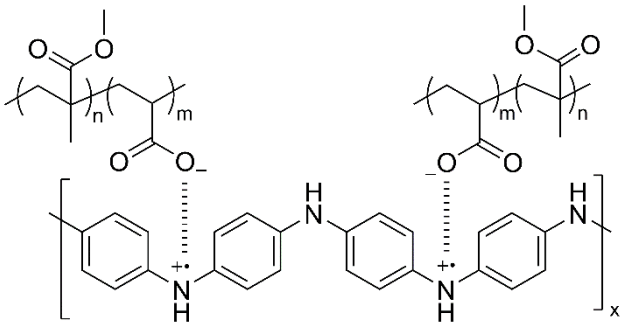

Figure 1. Schematic representation of electrostatic interaction between PMMA-*b*-PAA and PANI.

Complete protonation of PANI is essential for an effective complexation, which in turn depends on the amount of deionized water in the system and hence the morphology. Partial protonation was observed at 29 wt % water content (see the Supporting Information) and above which complete protonation was confirmed by UV-visible absorption spectrum. Experiments were performed at fixed 50 wt % water content, and their aggregate morphologies were studied at different block copolymer/homopolymer compositions. Formation of these complex aggregates resulted in a turbid solution.

Electrostatic interaction

The complexation between PANI and PMMA-*b*-PAA was due to electrostatic interaction between carboxylic acid groups (-COOH) of PAA and imine (=N-) groups of PANI. The imine sites of PANI are protonated in the acidic medium i.e. PANI-EB was oxidized to emeraldine salt form to acquire a positive charge on its backbone that induce attraction with negatively charged carboxylic acid groups.[22] A bathochromic shift of the absorption bands i.e. a shift towards higher wavelength was observed for complexes in UV-visible spectrum as a result of extended conjugation due to protonation (Figure 2).

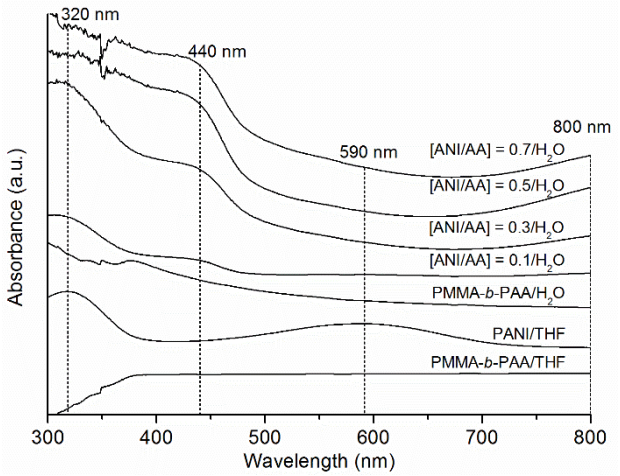

Figure 2. UV-visible spectra of PMMA-*b*-PAA, PANI in THF and PANI/PMMA-*b*-PAA complexes at [ANI]/[AA] = 0, 0.1, 0.3, 0.5, 0.7 in water.

For PANI-EB, the characteristic peak for π-π* electronic transition of the benzenoid segments and the exciton absorption band were observed at 320 nm and 590 nm respectively.[37] The doped or protonated form of PANI after complexation shows π-π* absorption band around 320 nm, a new polaron band around 440 nm and a bipolaron band around 800 nm (Figure 2). The complete protonation of PANI can be evidenced from the disappearance of exciton band and appearance of polaron and bipolaron bands at higher wavelengths. These absorption bands are identical to that of emeraldine salt (oxidized) form of PANI.[38] Furthermore, a visual indication of colour change from blue (Figure 3 a) for PANI-EB to dark green (Figure 3 c) for PANI/PMMA-*b*-PAA has been observed. Aggregation of pure block copolymer in absence of PANI resulted in a white turbid solution (Figure 3 b).

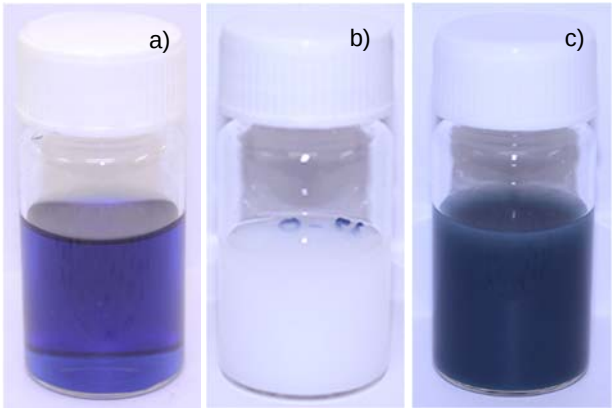

Figure 3. Photographs of a) PANI-EB in THF, b) PMMA-*b*-PAA aggregates and c) PANI/PMMA-*b*-PAA complexes in water.

The electrostatic complexation between PANI and PAA was analyzed by FTIR spectroscopy. The C-O, C=O stretching bands in PAA and –C=N, C=C stretching bands in PANI are particularly sensitive for ionic bonding during complexation. For pure PMMA-*b*-PAA block copolymer, the intense and broad band at 1735 cm^{-1} represents C=O stretching in PAA overlapped with PMMA carbonyl groups. The broadening of carbonyl stretching may be attributed to the presence of inter/intramolecular hydrogen bonding (OH·····O-C) and free carbonyl groups. The C-O stretching was observed at 1389 cm^{-1} as a weak band. After complexation, bands corresponding to C=O and C-O were shifted to lower wavenumbers, namely 1730 cm^{-1} and 1386 cm^{-1} for [ANI]/[AA] = 0.7 due to ionic bonding[39] (Figure 4). Here, the C=O stretching bands appear to be sharp and intense due to increasing in free carbonyl groups after complexation. Kanis et al.[40] reported similar behaviour for PEO/Carbopol blends and Akiba et al.[41] for P(S-co-MAA)/PEG blends. In pure PANI, the –C=N stretching bands of quinoid rings and C=C stretching bands of benzenoid rings observed at 1595 cm^{-1} and 1504 cm^{-1} were found to shifted to 1592 cm^{-1} and 1497 cm^{-1} (Figure 4) respectively after complexation.[42]

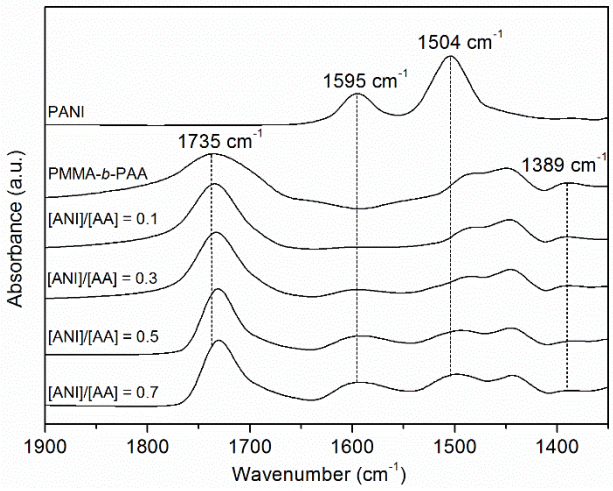

Figure 4. FTIR spectra showing the carbonyl stretching region of PMMA-*b*-PAA along with PANI and PANI/PMMA-*b*-PAA complexes.

Morphology of PANI/PMMA-*b*-PAA complexes in water

Block copolymers self-assemble into various morphologies in block selective solvents. Morphologies of these self-assembled aggregates are proven to depend on various factors such as polymer architecture, solvent compositions, additives, etc. Various additives from small molecules to flexible coil like homopolymers were selectively complexed with block copolymers and morphology transformations were studied.[33] In this study, PMMA-*b*-PAA block copolymer self-assembly in aqueous solution in the presence of a hydrophobic rod-like homopolymer PANI was reported. The water content during complex preparation was fixed at 50 wt % at which complete complexation was proven by UV-visible spectroscopy.

The morphologies of the aggregates were characterized using TEM and AFM measurements. Figure 5a and b shows the AFM and TEM images of spherical micellar aggregates prepared from pure PMMA-*b*-PAA block copolymer respectively. The hydrophobic PMMA block precipitates as core while the water

soluble PAA block forms corona upon water addition to THF/polymer solution. The morphology of self-assembled aggregates at particular water content depends on the degree of polymerization of the individual blocks, nature of the common solvent, presence of additives and polymer concentration. Here, the length of water soluble PAA block in PMMA-*b*-PAA block copolymer was long enough (mole fraction of PAA = 21.9%), which led to formation spherical micelles.[43] Figure 5a shows AFM height image of PMMA-*b*-PAA micelles as spherical structures with uniform size distribution. The hydrodynamic diameter (D_h) measured using DLS measurements shows a narrow peak with an average diameter of 49 nm (Figure 5 c). In addition to AFM and DLS results, the TEM images (Figure 5b) also shows spherical micelles of uniform size. The coronal PAA chains of micelles in TEM images appear dark due to uranyl acetate negative staining, while the higher electron transmission areas in the centre denotes PMMA core. Spherical micelles were the only observed morphology for pure block copolymer in aqueous solution.

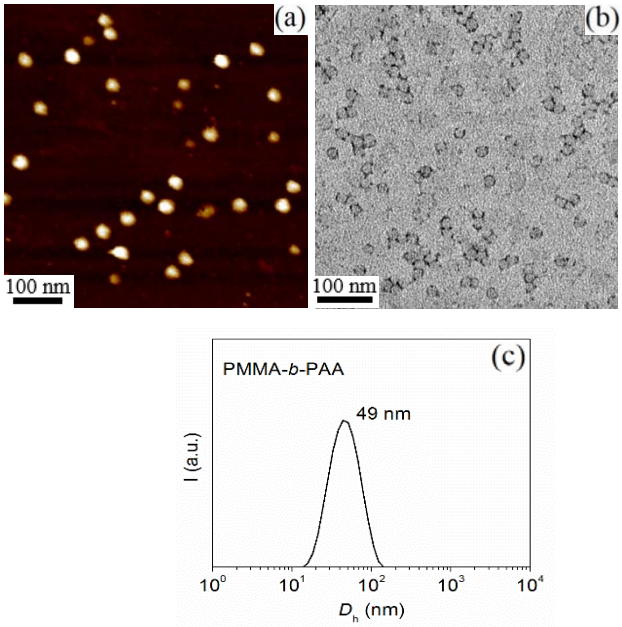

Figure 5. (a) AFM image and (b) TEM image of micelles, along with (c) hydrodynamic diameter (D_h) of PMMA-*b*-PAA block copolymer in water.

The morphology transformation was studied upon increasing PANI content. At very low PANI contents, i.e., at [ANI]/[AA] < 0.1, no change in morphology was observed. PANI may be adsorbed onto the coronal chains, but failed to tune the intrinsic self-assembling properties of the block copolymer owing to its lower concentration. Upon further increasing PANI content, figure 6 - 9 shows morphology transformation of aggregates from micelles to irregular vesicles through various intricate morphologies. PANI complexation with PAA through electrostatic interaction produced the morphology change with the change in the composition.

Figure 6 shows the morphology of self-assembled complexes at molar ratio of complexing units [ANI]/[AA] = 0.1. Vesicles were found to co-exist with micelles at this molar ratio. The AFM image (Figure 6 a) shows ring-like structures along with spherical dots that can be correlated to vesicles and micelles respectively. It implies that, fraction of PMMA-*b*-PAA block copolymer complexed with hydrophobic PANI self-assembled into vesicles as the block composition was altered. We assume that, hydrophobic PMMA chains form vesicle wall while the water soluble PAA chains form inner and outer corona. The PAA/PANI complex may be trapped at the core-solvent interface. In TEM image (Figure 6 b), the vesicle wall is transparent for electrons, while coronal chains appears dark due to staining. It can be noticed that these vesicles possess thin walls with larger cavity size. This behaviour was consistent with previous studies showing larger cavity size for polymer containing longer hydrophilic block.[44] The average wall thickness was measured to be approximately 22±2 nm and 25±3 nm from AFM and TEM images respectively. Two distinct narrow peaks at 43 nm and 220 nm in DLS measurement can be correlated to the D_h of micelles and vesicles respectively. Two distinct peaks give a clear indication of coexistence of homogeneous populations of micelles and vesicles (Figure 6 c).

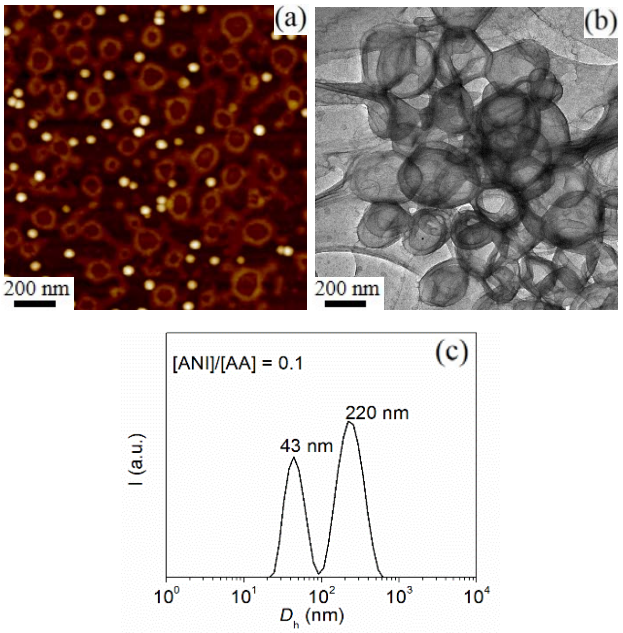

Figure 6. (a) AFM image and (b) TEM image of coexisted micelles and vesicles, along with (c) hydrodynamic diameter (D_h) at [ANI]/[AA] = 0.1 in water.

Even at higher PANI content [ANI]/[AA] = 0.3, micelles started sticking onto inner corona of the vesicles as seen in AFM and TEM images (Figure 7 a, b). In addition, the vesicles show an increase in size and wall thickness, hence the name thick walled vesicles (TWVs). An increase in overall wall thickness can be noticed from AFM (~ 40±3 nm) and TEM (~ 46±3 nm) images. The AFM image shows a broad size distribution of vesicles with

micelles appearing in the inner rim of vesicle walls. PANI complexes can be seen as gradient dark rings in TEM image as OsO4 stain attacks the amide bonds in PANI and gives higher contrast (Figure 7 b).[45] A distinct population of micelles were absent in both AFM and TEM images, which is confirmed from a single broad peak observed (at 232 nm) in DLS measurement (Figure 7 c).

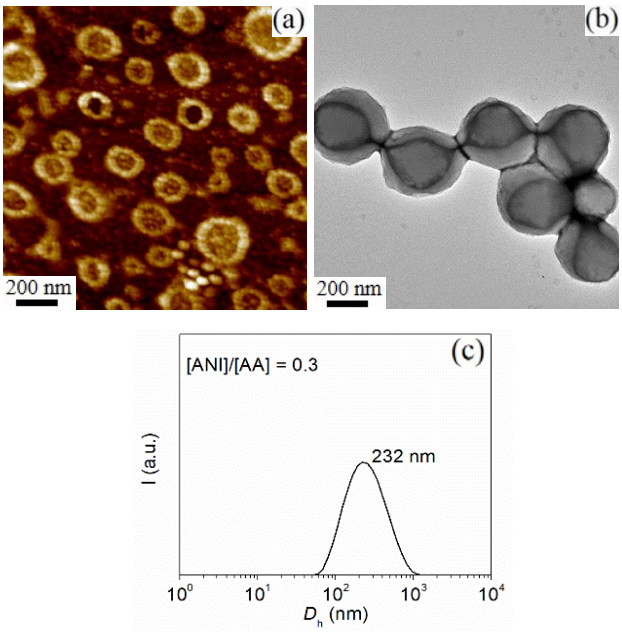

Figure 7. (a) AFM image and (b) TEM image of thick walled vesicles (TWVs), along with (c) hydrodynamic diameter (D_h) at [ANI]/[AA] = 0.3 in water.

Further increasing PANI content to [ANI]/[AA] = 0.5, micelles are found to be entrapped inside the vesicles resulting in a new morphology of MMVs. The entrapment efficiency is found to be much pronounced at higher water contents (>29 wt %) may be due to efficient complexation. Figure 8a shows the AFM height image of multimicellar vesicles, where spherical micelles are encapsulated inside the ring like vesicle wall. In TEM image, micelles coated with PANI appears as dark spheres inside the vesicles (Figure 8b). Here, PANI may act as bridging units between micelles through electrostatic complexation among the coronal chains leading to a compound vesicle. Compared to TWVs, MMVs exhibit a narrow DLS peak indicating a narrow size distribution as evidenced from TEM and AFM images. From DLS measurement, the average size (D_h) of vesicles was 396 nm showing an enormous increase in vesicle size.

At [ANI]/[AA] = 0.7 and higher PANI contents, the complex aggregates started forming macroscopic precipitates in aqueous solution. Precipitation may be due to vesicle aggregation as the solvent (water) is unfavourable for hydrophobic PANI component. This condition drove formation of irregular vesicles along with PANI clusters can be observed from the AFM and TEM images (Figure 9a, b). A broad bimodal DLS peak centring on 352 nm denotes inhomogeneous hydrodynamic size distribution of vesicles (Figure 9c).

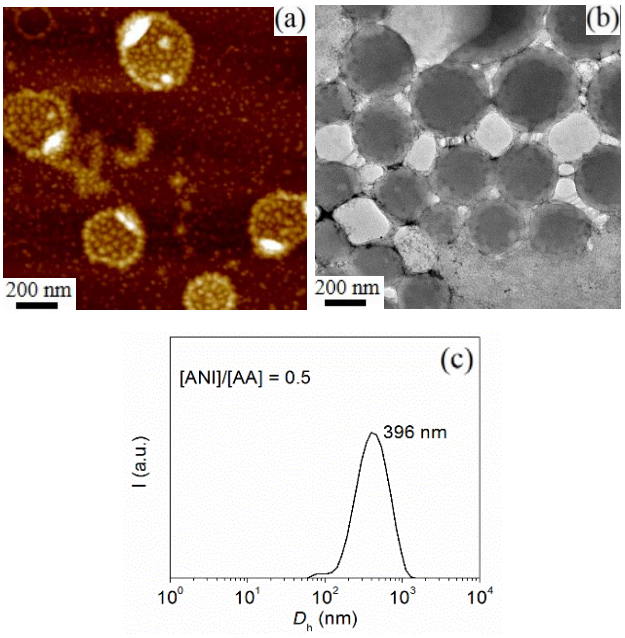

Figure 8. (a) AFM image and (b) TEM image of multimicellar vesicles (MMVs), along with (c) hydrodynamic diameter (D_h) at [ANI]/[AA] = 0.5 in water.

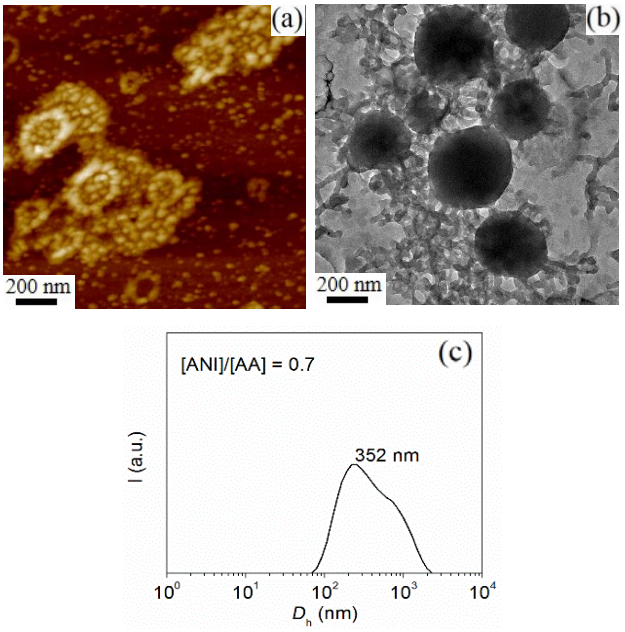

Figure 9. (a) AFM image and (b) TEM image of irregular vesicles, along with (c) hydrodynamic diameter (D_h) at [ANI]/[AA] = 0.7 in water.

Morphology transformation of aggregates

Block copolymers can self-assemble into various morphologies in solution depending on the polymer composition and distinct

interaction with additives and solvents. Secondary interactions such as electrostatic interaction and hydrophobic interaction can be exploited to tune the morphology of self-assembled aggregates through complexation.[35] In this study, electrostatic interaction between PAA and PANI tunes morphology of aggregates at various molar ratios which is entirely different form the morphologies observed for pure block copolymer. Since ionization of weak polyacid such as PAA is sensitive to solvent composition, experiments were performed at 50 wt % water content where protonation of PANI was complete.

The schematic diagram in figure 10 shows the morphology transformation at various PANI contents as observed in TEM and AFM images. The equilibrium morphology of any self-assembled block copolymers in solution depend on three contributions to the free energy of the system: core chain stretching, core-solvent interaction and inter coronal repulsion.[46] For amphiphilic block copolymers, the equilibrium morphology depends on hydrophilic/hydrophobic ratio '*f*' that directly affects free energy contributions of the system. Eisenberg et al. reported formation of spherical micelles in amphiphilic block copolymers when the mole percentage of hydrophilic block is $\geq$ 9.5.[36] PMMA-*b*-PAA block copolymer used in this study with PAA mole percent 21.9 resulted in spherical micelles as expected. Water addition to polymer/THF solution resulted in PMMA precipitation to form micellar core, while the water soluble PAA forms corona. Upon adding PANI to PMMA-*b*-PAA, vesicles were formed along with micelles at [ANI]/[AA] = 0.1. Similar behaviour was reported in surfactant containing block copolymer system where mixed morphologies were observed at various surfactant contents.[47] Due to PANI/PAA complexation, PANI may reduce the intercoronal repulsion among partially ionized PAA chains due to shielding of electric charges. This situation is similar to a reduction in PAA chain length which may lead to increase in aggregation number N_{agg} and core chain stretching in order to decrease the interfacial energy between the core and the solvent. For block copolymers with relatively long hydrophilic block like this, the intercoronal repulsion plays important role than the core chain stretching in determining final morphology.[13] In order to reduce the free energy of the system and avoid entropic penalty associated with PMMA chain stretching, the micellar aggregates may be transformed into vesicular structures with increased overall size. In addition to above-mentioned free energy contributions, rod-like conjugated polymers have entropic penalty associated with π-stacking[23] of polymer chains may control morphology of these aggregates.

At [ANI]/[AA] = 0.3, thick walled vesicles (TWVs) were observed with increased overall size. Fraction of PAA chain undergone complexation with PANI may be segregated as inner corona, while free PAA chains with higher water solubility forms outer corona. The increase in PANI accumulation over the core-solvent interface may be correlated to increase in vesicle wall thickness. Similar phenomenon was observed in block copolymer complexes through hydrogen bonding by Salim et al.[48] As seen from AFM and TEM micrographs (Figure 7a, b) higher PANI content inside vesicles facilitated PANI coated micelles to stick onto the inner coronal walls. The overall size and vesicle wall thickness seems to increase with increasing PANI content.

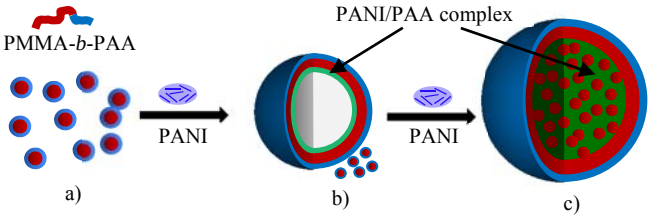

Figure 10. Schematic representation of morphology transformation in PMMA-*b*-PAA/PANI complexes. a) PMMA-*b*-PAA micelles, b) coexistence of micelles and vesicles at [ANI]/[AA] = 0.1 and c) multimicellar vesicle at [ANI]/[AA] = 0.5.

Multimicellar vesicles were observed at [ANI]/[AA] = 0.5. We assume that micelles with PANI saturated corona were trapped inside the vesicles during aggregation. As number of previous studies suggests,[49-51] complex structures can be observed through block copolymer self-assembly in presence of small molecules or homopolymers that have preferential interaction with one of the blocks of block copolymer. In the same vein, PANI having preferential interaction with PAA would help in bridging coronal chains of neighbouring micelles to from MMVs. In addition to bridging, PANI chains can stalk to form PANI bundles since aromatic units in PANI can stack via secondary forces and π interaction. These PANI bundles may help the formation of MMVs by sticking micelles together. In other words, preformed PANI/PAA complexes at this higher PANI content may have limited time for polymer chain rearrangement in the experimental time scale may have resulted in micelle entrapped vesicles. The corona repulsion among the PAA chains is diminished at higher PANI content, which flock micelles together and precipitate inside the vesicles. The free PAA chains can for hydrogen bonding with water, hence providing water solubility for the aggregates. At much higher PANI content [ANI]/[AA] = 0.7, irregular aggregates were observed presumably due to over saturation of PANI among the corona forming PAA chains that hinders solubility. The complexes started precipitating above [ANI]/[AA] = 0.5 as the hydrophobic PMAA and PANI content increases in solution. The PANI bundles formed in addition to complexes resulted in the formation of macroscopic aggregates. It can be concluded that, electrostatic interaction between PANI and PAA brought the morphology transformation in aggregates.

Conclusions

This study reports the self-assembly behaviour of PMMA-*b*-PAA block copolymer in the presence of a rigid rod homopolymer PANI. We have showed that morphology of self-assembled coil like block copolymer can be tuned via adding minor quantities of rigid homopolymer having specific interaction with either of the blocks of block copolymer. Morphology transformation at various PANI/PAA molar ratios

was driven by electrostatic interaction between PANI and PAA block of the block copolymer. A variety of morphologies such as micelles, vesicles, thick-walled vesicles (TWVs), multimicellar vesicles (MMVs) and irregular vesicles were observed upon increasing [ANI]/[AA] from 0.1 to 0.7. Micelle entrapped vesicles i.e. multimicellar vesicles; a new morphology was observed at [ANI]/[AA] = 0.5 through PANI complexation. This simple and effective way of micellar encapsulation may find interesting applications in nanotechnology.

Acknowledgment

A P was supported by Deakin University Postgraduate Research Scholarship (DUPRS).

Notes and references

Polymers Research Group, Institute for Frontier Materials, Deakin University, Locked Bag 2000, Geelong, Victoria 3220, Australia. E-mail: qguo@deakin.edu.au

† Electronic Supplementary Information (ESI) available: The UV-visible spectrum of complexes at 29 wt % water content along with photographs of complexes at various PANI content are presented in this section. See DOI: 10.1039/b000000x/

1. D. E. Discher and A. Eisenberg, *Science*, 2002, **297**, 967-973.
2. G. Gaucher, M.-H. Dufresne, V. P. Sant, N. Kang, D. Maysinger and J.-C. Leroux, *J. Control. Release.*, 2005, **109**, 169–188.
3. I. W. Hamley, *Angew. Chem., Int. Ed.*, 2003, **42**, 1692–1712.
4. G. Riess, *Prog. Polym. Sci.*, 2003, **28**, 1107–1170.
5. G. Verma and P. A. Hassan, *Phys. Chem. Chem. Phys.*, 2013, **15**, 17016-17028.
6. T. Azzam and A. Eisenberg, *Angew. Chem. Int. Ed.*, 2006, **45**, 7443–7447.
7. E. Yoshida, *Supramol. Chem.*, 2014, DOI: 10.1080/10610278.10612014.10959014.
8. E. Yoshida, *Colloid Polym. Sci.*, 2014, **292**, 2555-2561.
9. E. Yoshida, *Colloid Polym. Sci.*, 2014, **292**, 763-769.
10. E. Yoshida, *Colloid Polym. Sci.*, 2014, **292**, 1463-1468.
11. K. Liu, Y. Kang, Z. Wang and X. Zhang, *Adv. Mater.*, 2013, **25**, 5530–5548.
12. A. Choucair and A. Eisenberg, *Eur. Phys. J. E*, 2003, **10**, 37-44.
13. L. Zhang and A. Eisenberg, *Macromolecules*, 1996, **29**, 8805–8815.
14. N. Hameed and Q. Guo, *Polymer*, 2008, **49**, 922-933.
15. A. Noro, Y. Sageshima, S. Arai and Y. Matsushita, *Macromolecules*, 2010, **43**, 5358–5364.
16. Q. Guo and H. Zheng, *Polymer*, 1999, **40**, 637-646.
17. J. Huang, X. Li and Q. Guo, *Eur. Polym. J.*, 1997, **33**, 659-665.
18. Q. Guo, *Macromol. Rapid Commun.*, 1990, **11**, 279-283.
19. N. Lefèvre, C.-A. Fustin and J.-F. c. Gohy, *Macromol. Rapid Commun.*, 2009, **30**, 1871–1888.
20. M. He, F. Qiu and Z. Lin, *J. Mater. Chem.*, 2011, **21**, 17039-17048.
21. M. A. Tracy and R. Pecora, *Annu. Rev. Phys. Chem.*, 1992, **43**, 525–557.
22. L. A. McCullough, B. Dufour and K. Matyjaszewski, *Macromolecules*, 2009, **42**, 8129–8137.
23. L. A. McCullough and K. Matyjaszewski, *Mol. Crystals Liq. Crystals.*, 2010, **521**, 1–55.
24. J. H. Cheung, W. B. Stockton and M. F. Rubner, *Macromolecules*, 1997, **30**, 2712-2716.
25. R. Nagarajan, W. Liu, J. Kumar, S. K. Tripathy, F. F. Bruno and L. A. Samuelson, *Macromolecules*, 2001, **34**, 3921–3927.
26. J. Rubio-Magnieto, A. Thomas, S. Richeter, A. Mehdi, P. Dubois, R. Lazzaroni, S. Clement and M. Surin, *Chem. Commun.*, 2013, **49**, 5483–5485.
27. L. Yan and W. Tao, *J. Polym. Sci., Part A: Polym. Chem.*, 2008, **46**, 12–20.
28. Z. Yang, J. Wu, Y. Yang, X. Zhou and X. Xie, *Front. Chem. Eng. China*, 2008, **2**, 85–88.
29. J. B. Gilroy, D. J. Lunn, S. K. Patra, G. R. Whittell, M. A. Winnik and I. Manners, *Macromolecules*, 2012, **45**, 5806–5815.
30. H. Wang and Y. Han, *Macromol. Rapid Commun.*, 2009, **30**, 521–527.
31. W. B. Stockton and M. F. Rubner, *Macromolecules*, 1997, **30**, 2717–2725.
32. T. Homma, M. Kondo, T. Kuwahara and M. Shimomura, *Polymer*, 2012, **53**, 223–228.
33. D. V. Pergushov, E. V. Remizova, J. Feldthusen, A. B. Zezin, A. H. E. Muller and V. A. Kabanov, *J. Phys. Chem. B*, 2003, **107**, 8093–8096.
34. M. Marguet, C. Bonduelle and S. Lecommandoux, *Chem. Soc. Rev.*, 2013, **42**, 512–529.
35. D. V. Pergushov, A. H. E. Muller and F. H. Schacher, *Chem. Soc. Rev.*, 2012, **41**, 6888–6901.
36. Y. Mai and A. Eisenberg, *Chem. Soc. Rev.*, 2012, **41**, 5969–5985.
37. S. A. Chen and H. T. Lee, *Macromolecules*, 1995, **28**, 2858–2866.
38. J. Luo, Q. Zhou, J. Sun, J. Jiang, X. Zhou, H. Zhang and X. Liu, *J. Polym. Sci. A Polym. Chem.*, 2012, **50**, 4037–4045.
39. X. H. Lu, C. Y. Tan, J. W. Xu and C. B. He, *Synt. Met.*, 2003, **138**, 429–440.
40. L. A. Kanis, F. o. C. Viel, J. n. S. Crespo, J. R. Bertolino, A. T. N. Pires and V. Soldi, *Polymer*, 2000, **41**, 3303–3309.
41. I. Akiba, Y. Ohba and S. Akiyama, *Macromolecules*, 1999, **32**, 1175–1179.
42. C. C. Yang, T. Y. Wu, H. R. Chen, T. H. Hsieh, K. S. Ho and C. W. Kuo, *Int. J. Electrochem. Sci.*, 2011, **6**, 1642–1654.
43. L. F. Zhang and A. Eisenberg, *Polym. Adv. Technol.*, 1998, **9**, 677-699.
44. L. Ma and A. Eisenberg, *Langmuir*, 2009, **25**, 13730–13736.
45. K. Desai C. and Sung, *NSTI Nanotech*, 2004, **4**, 429 – 432.
46. L. F. Zhang and A. Eisenberg, *J. Am. Chem. Soc.*, 1996, **118**, 3168–3181.
47. S. E. Burke and A. Eisenberg, *Langmuir*, 2001, **17**, 8341-8347.
48. N. V. Salim and Q. Guo, *J. Phys. Chem. B*, 2011, **115**, 9528–9536.
49. N. V. Salim, N. Hameed, T. L. Hanley, L. J. Waddington, P. G. Hartley and Q. Guo, *Langmuir*, 2013, **29**, 9240–9248.
50. J. Zhu, S. Zhang, K. Zhang, X. Wang, J. W. Mays, K. L. Wooley and D. J. Pochan, *Nat. Commun.*, 2013, **4**, 2297.
51. A. Palanisamy and Q. Guo, *J. Phys. Chem. B*, 2014, DOI: 10.1021/jp508352a.

